ADVANCED MATERIALS INTERFACES
Open Access

Supporting Information

for *Adv. Mater. Interfaces*, DOI 10.1002/admi.202400085

Impact of Band-gap Gradient in Semi-Transparent and Bifacial Ultra-Thin Cu(In,Ga)Se_2 Solar Cells

*Christoph Rath, Yao Gao, Tristan Koehler and Martina Schmid**

Supporting Information

Impact of Band Gradient in Semi-transparent and Bifacial Ultra-thin Cu(In,Ga)Se_2 Solar Cells

Christoph Rath[§]*, Yao Gao*[§]*, Tristan Koehler and Martina Schmid**

Department of Physics and Center for Nanointegration Duisburg-Essen (CENIDE)

University of Duisburg-Essen

Forsthausweg 2, 47057 Duisburg, Germany

* E-mail: martina.schmid@uni-due.de

§ Christoph Rath and Yao Gao contributed equally to this work.

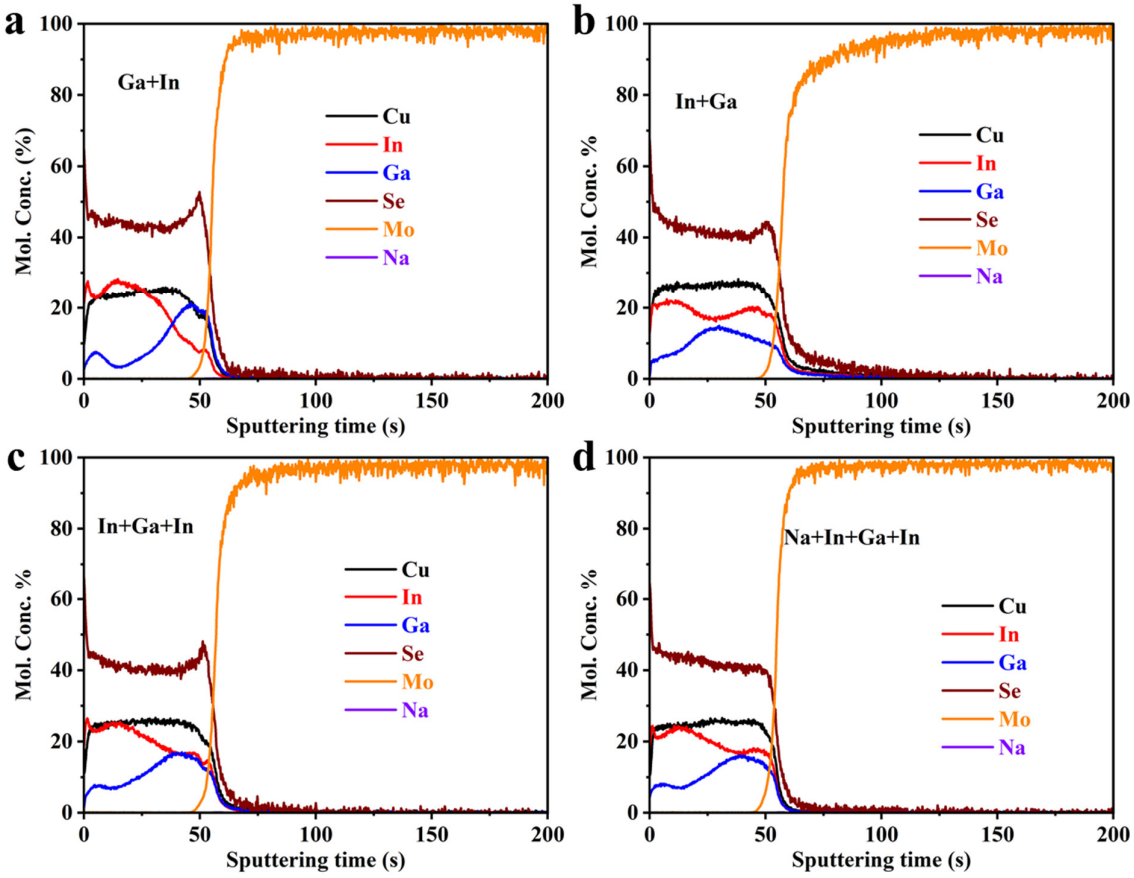

Figure S1. Composition depth profiles of CIGSe absorbers on Mo back contact with various deposition strategies in the first stage as measured by GD-OES. (a) Ga+In CIGSe, (b) In+Ga CIGSe, (c) In+Ga+In CIGSe, and (d) Na+In+Ga+In CIGSe. All these measurements were carried out after removing the excess Na by etching in 10% HCl solution for 2 min.

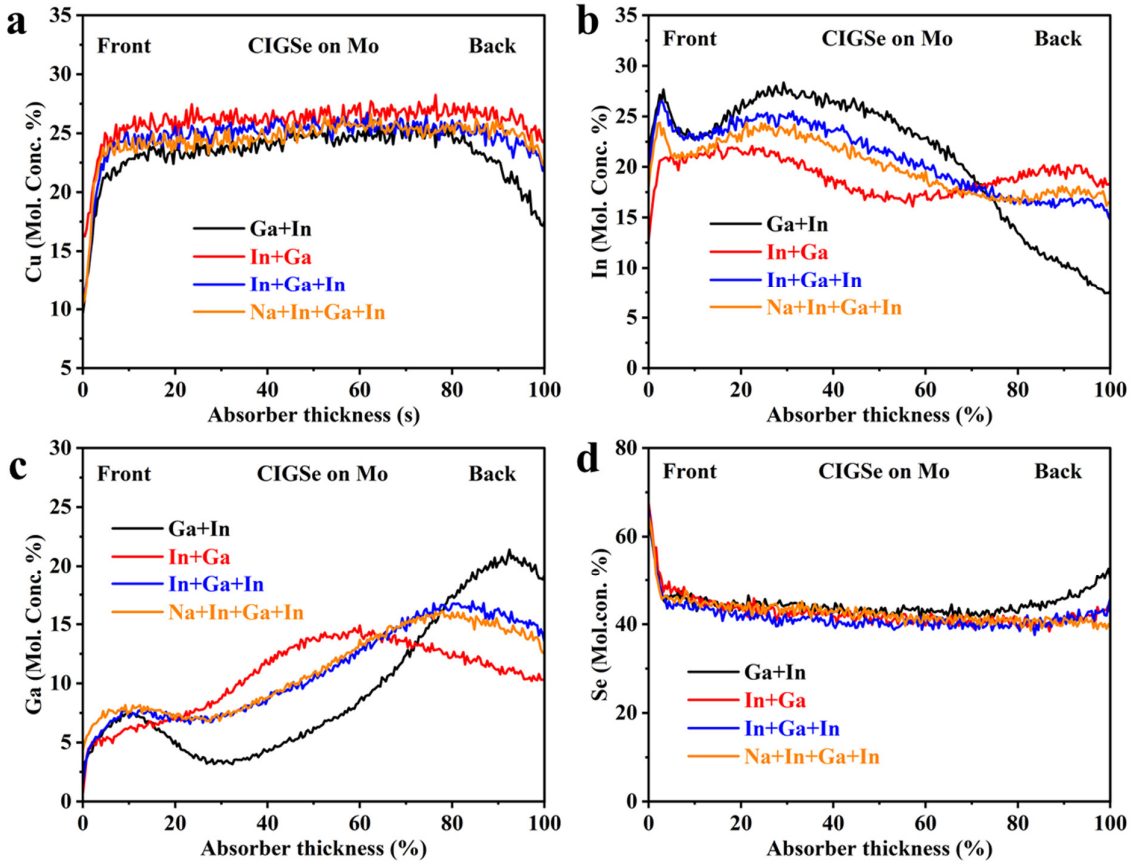

Figure S2. Elemental distribution of CIGSe absorbers on Mo back contact with various deposition strategies in the first stage as measured by GD-OES. (a) Cu, (b) In, (c) Ga, and (d) Se. The *x*-axis is normalized to 100% absorber thickness.

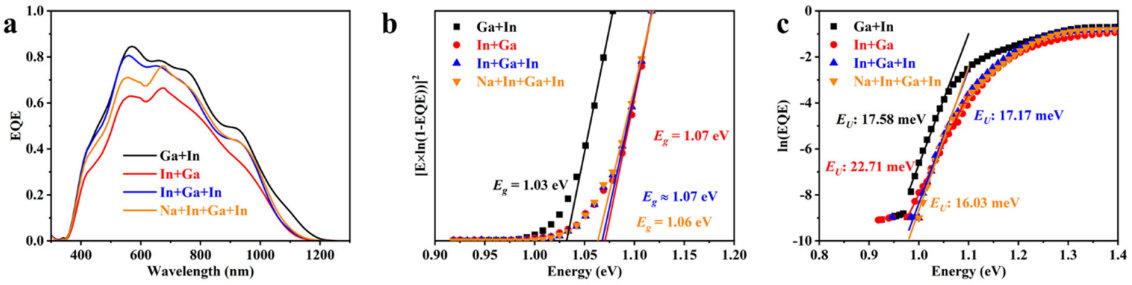

Figure S3. (a) External quantum efficiency, (b) bandgap extraction, (c) ln(EQE) as a function of photon energy at the long-wavelength edge to determine the Urbach energy E_U for the best-performing devices.

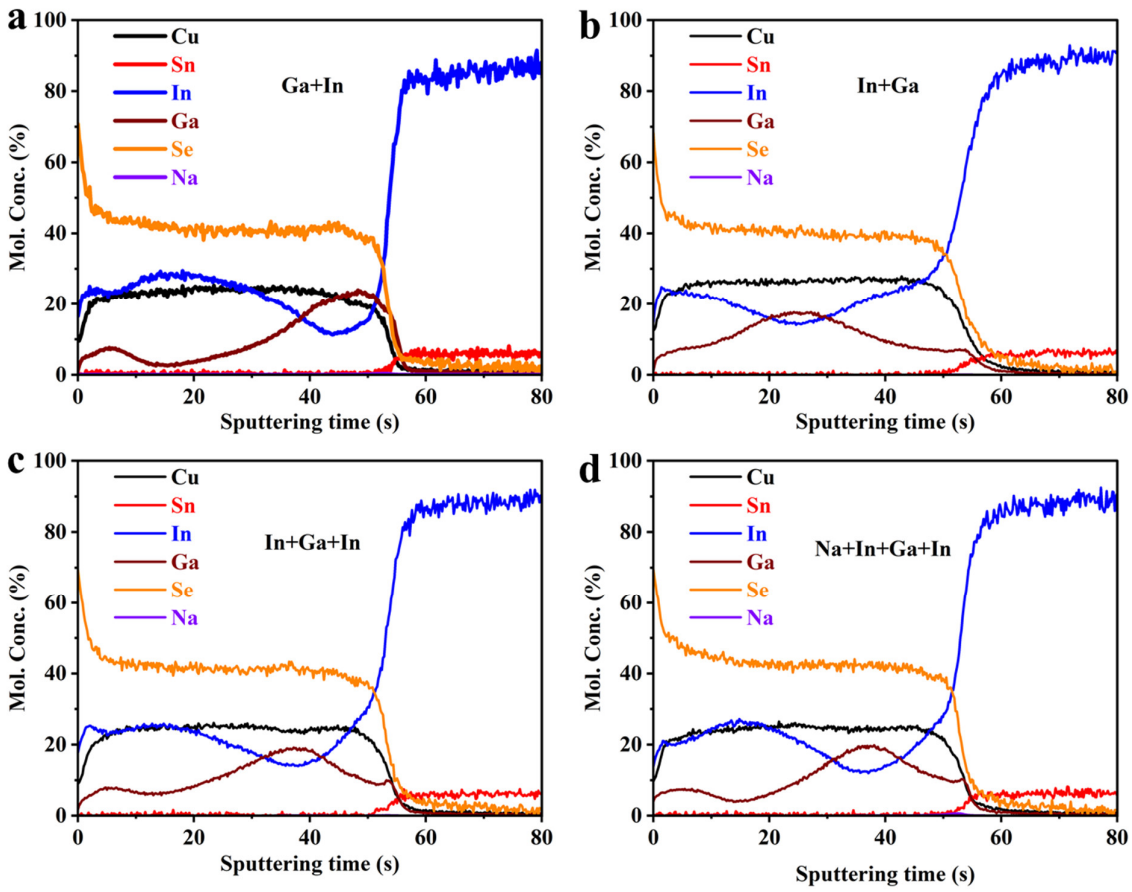

Figure S4. Composition depth profiles of CIGSe absorbers on ITO back contact with various deposition strategies in the first stage as measured by GD-OES. (a) Ga+In CIGSe, (b) In+Ga CIGSe, (c) In+Ga+In CIGSe, and (d) Na+In+Ga+In CIGSe. All these measurements were carried out after removing the excess Na by etching in 10% HCl solution for 2 min.

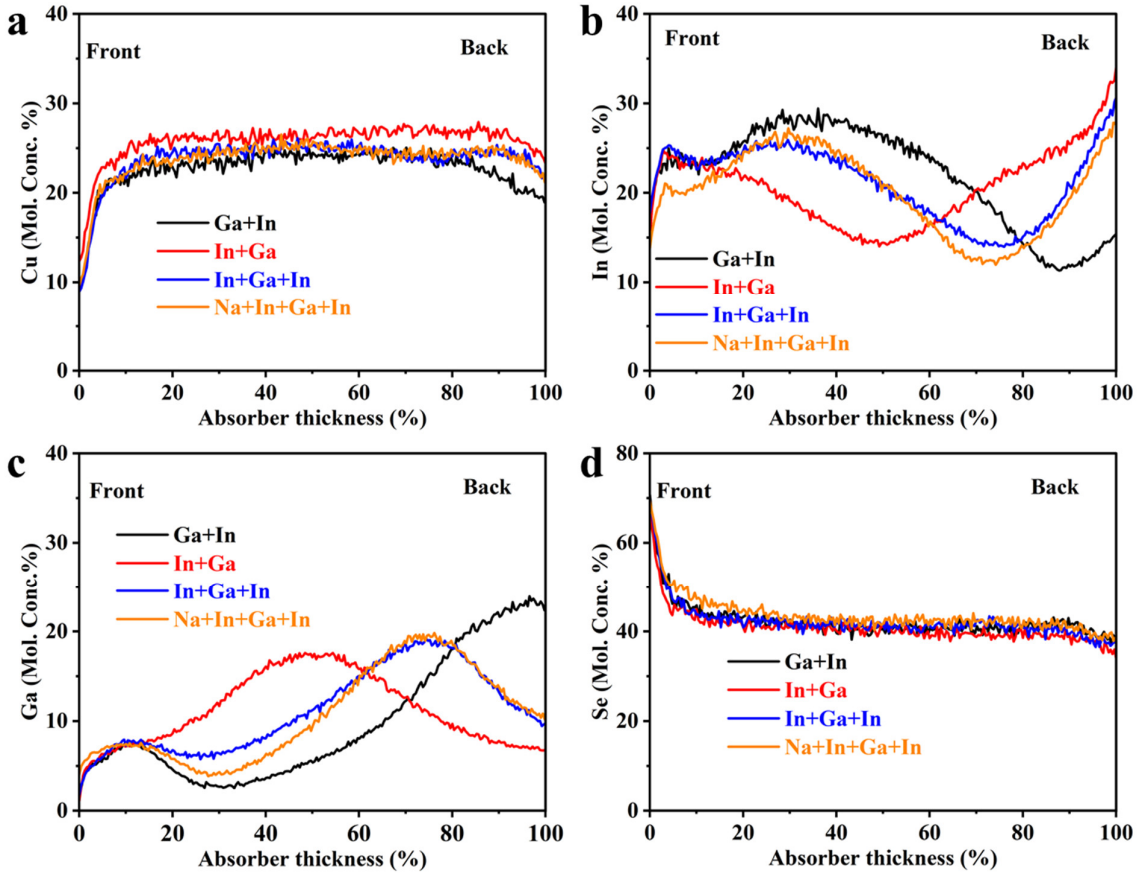

Figure S5. Elemental distribution of CIGSe absorbers on ITO back contact with various deposition strategies in the first stage as measured by GD-OES. (a) Cu, (b) In, (c) Ga, and (d) Se. The *x*-axis is normalized to 100% absorber thickness.

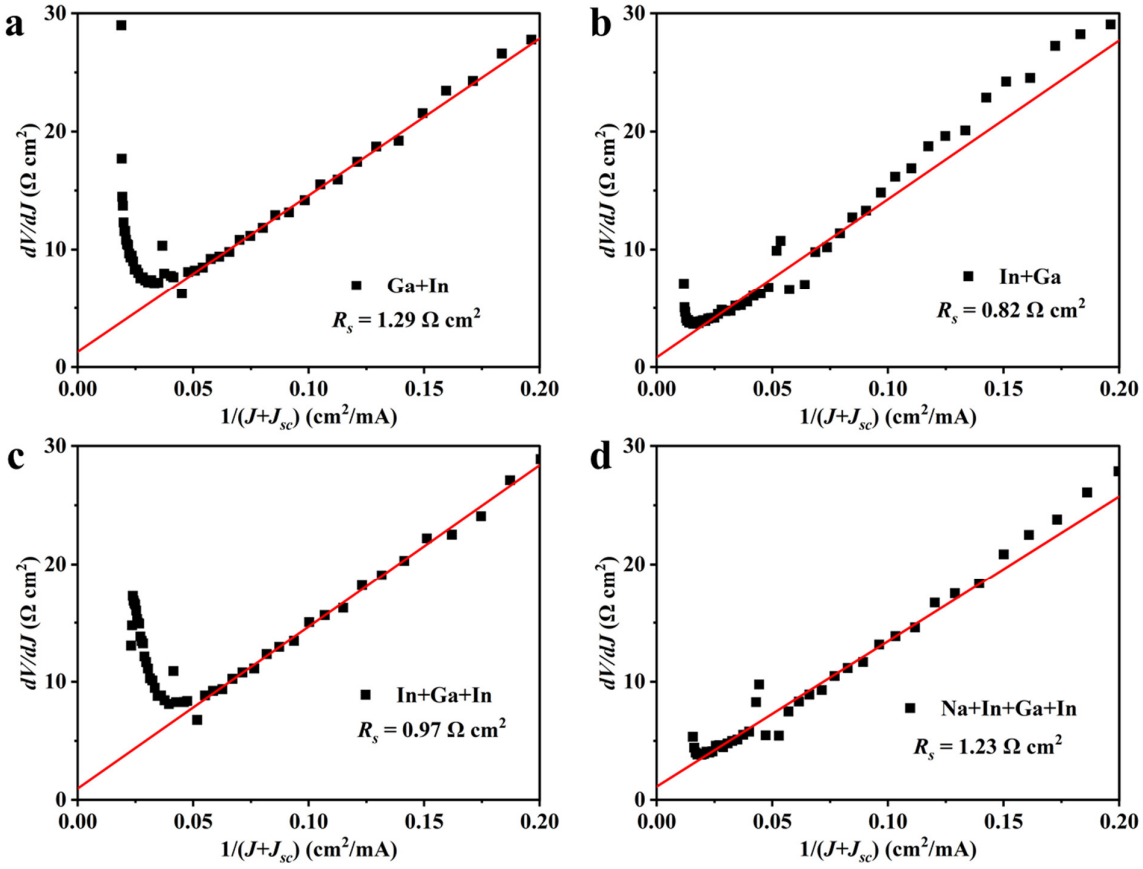

Figure S6. Determination of series resistance (R_S) for ultra-thin CIGSe absorbers deposited on ITO back contact with various deposition strategies in the first stage.

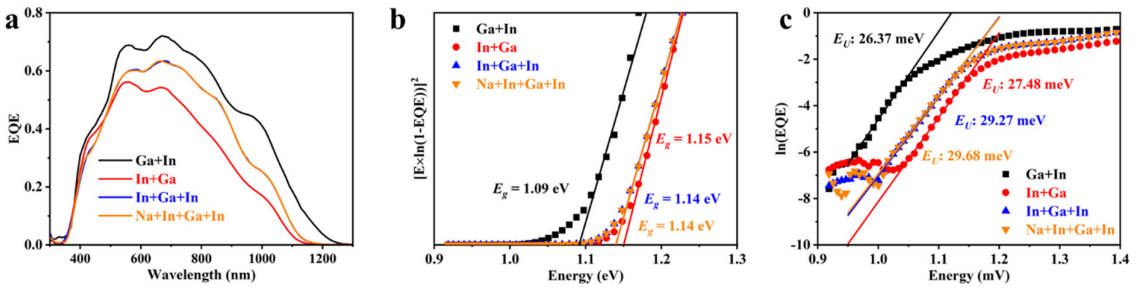

Figure S7. (a) External quantum efficiency, (b) bandgap extraction, and (c) ln(EQE) as a function of photon energy at the long-wavelength edge to determine the Urbach energy E_U for the best-performing devices.

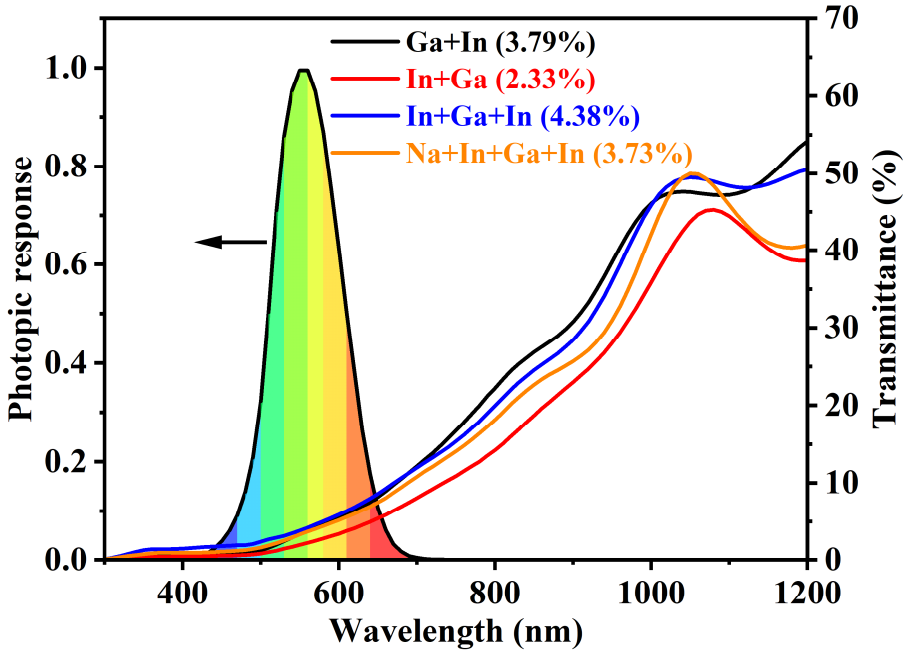

Figure S8. The photopic response curve of the human eye and transmittance profiles for the semitransparent ultra-thin CIGSe devices with various deposition strategies in the first stage (average visible transmittances for each device in the spectral range of 380-770 nm are enclosed in the brackets).